Catalysis Today 172 (2011) 158–165

Contents lists available at ScienceDirect

Catalysis Today

journal homepage: www.elsevier.com/locate/cattod

CO_2 capture *via* catalytic hydrogenation to methanol: Thermodynamic limit vs. 'kinetic limit'

Esteban L. Fornero, Dante L. Chiavassa, Adrian L. Bonivardi, Miguel A. Baltanás*

INTEC, Instituto de Desarrollo Tecnológico para la Industria Química (Universidad Nacional del Litoral and CONICET), Güemes 3450, S3000GLN Santa Fe, Argentina

ARTICLE INFO

Article history:
Received 29 November 2010
Received in revised form 11 February 2011
Accepted 14 February 2011
Available online 1 April 2011

Keywords:
Carbon dioxide
Capture
Methanol
Fixed-bed catalytic reactors

ABSTRACT

The production of methanol *via* the catalytic hydrogenation of carbon oxides was simulated in a reacting system that included the recycling of noncondensable gases (H_2, CO_2 and CO) to evaluate the CO_2 capture capability of the process. As a first step, the asymptotic responses of the system 'operating in thermodynamic equilibrium' (i.e., overall recoveries of CO_2 and H_2, CH_3OH selectivity and productivity) were analyzed for various industrial conditions of pressure (3–5 MPa), temperature (508–538 K), feed composition (H_2/CO_2 = 1.5/1 to 4/1) and mole recycle ratio (R) with respect to the molar feed flow rate. Then the performance of two catalysts (a novel one, Pd–Ga_2O_3/SiO_2 and a commercial $CuO/ZnO/Al_2O_3$ type) in an ideal isothermal, isobaric, pseudohomogeneous fixed-bed reactor was studied for a broad range of W/F_{CO_2} ratios.

It was found that, whereas the 'reactor in equilibrium' would allow up to 100% CO_2 capture, the capture values upon using these catalysts were significantly lower. Nevertheless, such recoveries always increased whenever R was raised, which implies that catalyst development efforts in this field should prioritize achievement of the highest catalytic activity (i.e., specific productivity) rather than attempt catalyst selectivity improvements.

1. Introduction

The concentration of CO_2 in the earth's atmosphere has reached its highest level in the past 500,000 years. From the beginning of the industrial era, the emission rates of carbon dioxide have steadily escalated. More recently – in particular since 2000 – the accumulation of this greenhouse gas has intensified. Consequently, the quest for, and the development of, processes aimed at mitigating the impact of the CO_2 generated by fossil fuel combustion, set free in the cement and steel industries, or released during natural gas extraction and commercialization activities, has become a priority.

The concept of recovery and recycling of CO_2 *via* the manufacture of products whose usage would imply lower greenhouse gas emissions is a compelling and viable option. Within this context fall the processes that resort to catalytic hydrogenation of carbon oxides for the manufacture of methanol and/or dimethylether (DME), whose technical feasibility has already been demonstrated in pilot plant and 'demo' scale developments by the RITE and KIST research teams [1–3]. Both products are of great interest because, among other uses, they can become a partial substitute for fossil fuels [4].

In this regard, the conventional Cu/ZnO catalysts that might be employed for these purposes are also extremely sensitive to poisons, which are usually present in point emission sources of CO_2 [5]. Non-conventional formulations using supported palladium (i.e., Pd/Ga_2O_3) have been shown to be more active and selective than the classical catalysts based on copper [6]. Yet, they invariably generate CO and water as the principal process byproducts, which, in turn, affect their catalytic activity, but not their stability [7].

Our research team recently developed a novel material, Ga_2O_3–Pd/SiO_2, which was shown to be very stable, active and selective to methanol using CO_2/H_2 mixtures [8,9]. Therefore, it could be potentially applicable for CO_2 capture on an industrial scale. However, because only integral reactors should be used in any practical process (and with recycling of non-condensable gases), the catalyst necessarily must be put in contact with a high concentration of potentially deleterious reaction products, among which CO and water stand out. Water can be eliminated prior to recycling by condensation, but the separation of CO is costly, and it is always present in the industrial effluents that would be used as reactor feed.

To duly assess the impact of the various process variables on the catalyst performance *via* numerical simulation, a *CO_2 capture module* was conceived. Two different catalysts will be examined in the present work: the novel material introduced above and a commercial one, both for the selective production of methanol by

* Corresponding author. Tel.: +54 342 455 9175; fax: +54 342 455 0944.
E-mail address: tderliq@santafe-conicet.gov.ar (M.A. Baltanás).

0920-5861/$ – see front matter © 2011 Elsevier B.V. All rights reserved.
doi:10.1016/j.cattod.2011.02.036

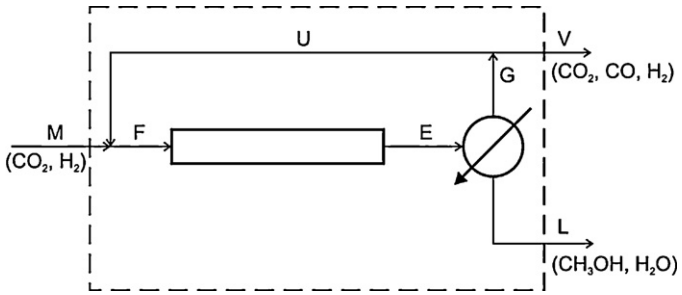

Fig. 1. Schematic of the CO_2 capture (methanol synthesis) module.

CO_2 hydrogenation in a continuous multitubular fixed-bed reactor operating in steady state. To simplify matters, the simplest ideal model will be considered, namely a pseudohomogeneous (1D), isothermal, isobaric reactor without inert gases in the feedstream, nor catalyst deactivation. Typical industrial process conditions will be analyzed (P = 3–5 MPa, T = 508–538 K) for H_2/CO_2 ratios of 1.5/1 to 4/1, making comparisons with the thermodynamic limit at each set of conditions. Indeed, given the characteristics of the reacting system (the main reaction is exothermic, with reduction in the number of moles of the reactants), this analysis constitutes then a 'best case scenario'.

The numerical simulation of reactors and processes allows for a rapid appraisal of their behavior without incurring costly experiments, and also serves to guide or focus future research. There are numerous works in this area, with different purposes and goals, such as the study of catalyst deactivation [10], comparison among different reactor models [11], or the optimization of the synthetic process [12]. Here we merely sought to obtain (albeit, exhaustively) the expected range of values of the percent capture of CO_2 from a point source, which is regarded as the priority variable in comparison with hydrogen use/recovery or catalyst productivity. Neither an optimization analysis nor the tackling of the economic aspects of the process itself was intended. Certainly, to *effectively* mitigate CO_2 emissions in energy saving terms, the hydrogen source to be used in the process must be of hydraulic, solar, or nuclear origin [2].

2. Process summary

2.1. Configuration of the CO_2 capture module

The CO_2 capture module consisted of an ideal multitubular fixed-bed reactor coupled to a total vapor condenser. The non-condensable gases (H_2, CO_2, and CO) were partially vented, but were mostly recycled by mixing them with the module feed stream, as outlined in Fig. 1. In the figure, M, F, E, G, U, V and L indicate the molar flow rates (mol/s) of module feed, reactor feed, reactor exit, non-condensable gases exiting from the condenser, non-condensable gases recycled to the reactor, gas vent, and condensed liquid (CH_3OH and H_2O) streams, respectively. From now on the quotient between the molar flow rate of non-condensable gases recycled to the reactor entrance with respect to the molar flow rate of gases fed to the system will be designated as the 'recycle ratio' (R):

$$R = \frac{U}{M} \quad \text{so that} \quad F = M(1+R)$$

The overall, independent reactions that take place in this reacting system whenever no appreciable production of DME or CH_4 occurs are the hydrogenation of CO_2, to produce methanol, and the reverse water gas shift reaction (RWGS):

$$CO_2 + 3H_2 \leftrightarrow CH_3OH + H_2O \quad (R_1)$$

$$CO_2 + H_2 \leftrightarrow H_2O + CO \quad (R_2)$$

The 'dry' reaction that produces methanol from carbon monoxide:

$$CO + 2H_2 \leftrightarrow CH_3OH \quad (R_3)$$

does not need to be taken into account in the thermodynamic calculations, as it can be expressed as a linear combination of the other two [9]. However, the *explicit* consideration of this reaction depended upon the kinetic expressions that have been reported for each catalyst type. In particular, only expressions corresponding to reactions (R_1) and (R_2) sufficed to describe the catalytic reactivity of our novel material [9]. Yet, for the commercial Cu-based catalyst that will be examined [13,14], the authors reported kinetic rate expressions for the full set of reactions ((R_1)–(R_3)) to fully explain the observed catalytic reactivity.

2.2. Thermodynamic limits of the process

A computer program was developed for calculating the steady-state composition of each of the module streams. The program, implemented in Digital Visual FORTRAN V 6.0 code, featured a numerical iterative algorithm where the inputs were, besides the thermodynamic database [15–17], the composition of the feed stream to the module (stream M) and the desired recycle ratio (R). From the mass balances in the first node, the feed composition to the reactor (stream F) was calculated by assuming a zero molar fraction of CO to initialize the iterative scheme. With the reactor feed composition, for any given values of temperature and pressure, the degrees of advancement at equilibrium of reactions (R_1) and (R_2) (ε_i^{EQ}) were then calculated by minimizing the total Gibbs free energy. It is worth mentioning that the use of fugacities, rather than partial pressures, was also considered, applying the Soave–Redlich–Kwong equation of state [15,18,19] the compressibility factors were never outside the 0.99–1.10 range and so using fugacities was found to give negligible changes in the results.

The exit molar fractions (y_j^E) of the 'equilibrium reactor' were then found for the complete set of fractional constricted approaches to equilibrium of (R_1) and/or (R_2) (λ_i, i = 1, 2) using the mass balance equations for each independent component:

$$y_j^E = \frac{1}{E}\left[F.y_j^F + \sum_{i=1}^{2} \upsilon_{ij}.\lambda_i.\varepsilon_i^{EQ}\right]$$

These fractional constrictions λ_i (which range between 0 and 1) constitute model parameters; υ_{ij} represents the stoichiometric coefficient for the ith reaction and the jth component. With the y_j^E values and the appropriate mass balances, the compositions of reactants and products in each stream were then recalculated until convergence was achieved (i.e., when the relative values of the concentration of CO at the exit of the 'reactor' (y_{CO}^E) between consecutive iterations was less than 1%).

2.3. The ideal catalytic reactor

The computer program used for simulating the steady-state operation of the capture module upon employing either catalyst was similar to the previous one. The former calculation of the equilibrium (or constrained equilibrium) composition of stream E was merely substituted by the calculation of the composition at the reactor exit resulting from the 'use' of each catalyst, as per the particular kinetics of each catalyst [9,13,14]. The calculation was done by solving, using the Gear method, the differential equations that

describe the mass balances of each independent component inside the pseudohomogeneous 1D reactor:

$$d(F.y_j^F) = \sum_{i=1}^{3} \upsilon_{ij}.r_i.dW \quad j = H_2,\ CO_2,\ CO,\ CH_3OH \ \text{ and } \ H_2O;$$

$$i = 1,\ 2\,(\text{or } 1,\ 2,\ 3\ -\ \text{see text}\ -)$$

where r_i is the specific reaction rate (mol/s kg catalyst) for the ith reaction. The iteration convergence criteria were the same as indicated above. Furthermore, for the purposes of this work, it was judged unnecessary to employ a heterogeneous reactor model as, for this synthesis, the overall yields found upon using more involved reactor models do not differ much with respect to those obtained by just using a homogenous model [11].

The kinetic expressions found using our novel, bifunctional Ga_2O_3–Pd/SiO_2 (2% Pd p/p, Ga/Pd = 3 at/at) catalyst were used first. The rate equations corresponding to (R_1) and (R_2) are the following [9]:

$$r_1 = \frac{k_1 p_{CO_2} p_{H_2} (1 - (p_{CH_3OH} p_{H_2O} / p_{H_2}^3 p_{CO_2} K_1))}{(1 + g_2.p_{CO_2} p_{H_2}^{0.5} + g_3.p_{CH_3OH} p_{H_2O} / p_{H_2}^2 + g_7.p_{H_2O} / p_{H_2}^{0.5} + g_9.p_{H_2}^{0.5})^2}$$

$$r_2 = \frac{k_2 p_{CO_2} p_{H_2}^{0.5} (1 - (p_{CO} p_{H_2O} / p_{H_2} p_{CO_2} K_2))}{(1 + g_2.p_{CO_2} p_{H_2}^{0.5} + g_3.p_{CH_3OH} p_{H_2O} / p_{H_2}^2 + g_7.p_{H_2O} / p_{H_2}^{0.5} + g_9.p_{H_2}^{0.5})}$$

in which K_i are equilibrium constants of reactions (R_1) and (R_2), p_i are partial pressures, k_i are the kinetic rate constants and g_i are chemisorption parameters of the model (their numerical values are given in Ref. [9]). The reaction rates were obtained by assuming a competitive chemisorption model between adsorbed atomic hydrogen, CO_2 and oxygenated intermediate species on the gallia surface, considering also that the rate-determining step (*rds*) of the synthesis reaction was the hydrogenation of the formate intermediate *and* that the carbon source for methanol was CO_2.

To compare the catalytic performance of this novel material with that of a 'benchmark' industrial catalyst, the kinetic expressions found by Graaf et al. [13,14], corresponding to commercial CuO/ZnO/Al_2O_3 (approximately 60/30/10 wt.%), were also used. On this catalyst, methanol can be synthesized simultaneously from CO_2 and CO. The rate-determining step for (R_1) and (R_2) was the hydrogenation of the methylenebisoxy intermediate, whereas upon CO chemisorption, the *rds* was the hydrogenation of surface formate [13]. The rate equations, corresponding to (R_1), (R_2) and (R_3), were thus the following:

$$r_1 = \frac{k_1 K_{CO_2} (f_{CO_2} f_{H_2}^{1.5} - f_{CH_3OH} f_{H_2O} / (f_{H_2}^{1.5} K_1))}{(1 + K_{CO} f_{CO} + K_{CO_2} f_{CO_2})(f_{H_2}^{1/2} + (K_{H_2O} / K_{H_2}^{1/2}) f_{H_2O})}$$

$$r_2 = \frac{k_2 K_{CO_2} (f_{CO_2} f_{H_2} - f_{CO} f_{H_2O} / K_2)}{(1 + K_{CO} f_{CO} + K_{CO_2} f_{CO_2})(f_{H_2}^{1/2} + (K_{H_2O} / K_{H_2}^{1/2}) f_{H_2O})}$$

$$r_3 = \frac{k_3 K_{CO} (f_{CO} f_{H_2}^{1.5} - f_{CH_3OH} / (f_{H_2}^{0.5} K_3))}{(1 + K_{CO} f_{CO} + K_{CO_2} f_{CO_2})(f_{H_2}^{1/2} + (K_{H_2O} / K_{H_2}^{1/2}) f_{H_2O})}$$

in which K_i are equilibrium constants, f_i are fugacities, k_i are kinetic rate constants, and K_{CO}, K_{CO_2}, K_{H_2O} and K_{H_2} are model parameters (their numerical values are given in Refs. [13,14]).

For whichever process condition was analyzed, and to visualize in more detail the performance patterns related to each catalyst, the same W/F_{CO_2} *per tube* corresponding to $R = 0$ was maintained in the module, regardless of which gas recycle ratio was considered afterwards. Of course, 'in practice' the use of a different R would imply having a different total number of tubes inside the reactor while keeping their length equal, but we found that this conceptual artifact allowed a simpler, isolated analysis of the impact of the W/F_{CO_2} variable on the catalyst performance. A set of extra simulations was done using the commercial catalyst of Graaf et al. [13,14] by keeping the same W/F_{carbon} per tube instead because, according to the kinetic rate expressions reported by these authors, CO was also an important reactant for CH_3OH synthesis by their catalytic material.

Table 1
Process conditions studied in the 'equilibrium reactor'.

Process condition	P (MPa)	T (K)	$[H_2/CO_2]_M$[a] (mol/mol)
E-1	3	523	75/25
E-2	4	523	75/25
E-3	5	523	75/25
E-4	3	523	80/20
E-5	3	523	70/30
E-6	3	523	60/40
E-7	3	508	75/25
E-8	3	538	75/25

[a] Stream M of the CO_2 capture module—see Fig. 1.

3. Results and discussion

To make quantitative comparisons among the different process conditions, the following definitions were employed:

- Overall module capture (OMC) of CO_2, % (CO_2 converted to CH_3OH):

$$OMC_{CO_2}\% = \frac{[My_{CO_2}^M - V(y_{CO_2}^V + y_{CO}^V)]}{My_{CO_2}^M} \times 100$$

- Percent of CO_2 converted to CO:

$$\%CO_2 \text{ to CO} = \frac{Vy_{CO}^V}{My_{CO_2}^M} \times 100$$

- Overall methanol selectivity (OMS) of the module, %:

$$OMS_{CH_3OH}\% = \frac{[My_{CO_2}^M - V(y_{CO_2}^V + y_{CO}^V)]}{(My_{CO_2}^M - Vy_{CO_2}^V)} \times 100$$

- Overall hydrogen capture (use) of the module, %:

$$OMC_{H_2}\% = \left[1 - \frac{Vy_{H_2}^V}{My_{H_2}^M}\right] \times 100$$

- Specific productivity to methanol (per unit mass of catalyst):

$$P_{CH_3OH} = \frac{Ly_{CH_3OH}^L (MW_{CH_3OH})}{W_{cat}} [=] \frac{\text{kg of } CH_3OH}{\text{kg cat. h}}$$

3.1. The 'equilibrium reactor'

Table 1 indicates the set of process conditions (pressure, temperature and feed composition) that were explored in the simulations. Both the overall module capture of carbon dioxide and the selectivity to methanol grow monotonically whenever R and/or λ_1 increased. As an example, Fig. 2 shows the obtained values of OMS_{CH_3OH}% for different gas recycle ratios (R) and different constriction settings for the chemical equilibrium of (R_1) (λ_1) while considering the RWGS in thermodynamic equilibrium ($\lambda_2 = 1$) using a stoichiometric H_2/CO_2 feed ratio at 3 MPa and 523 K. Under these

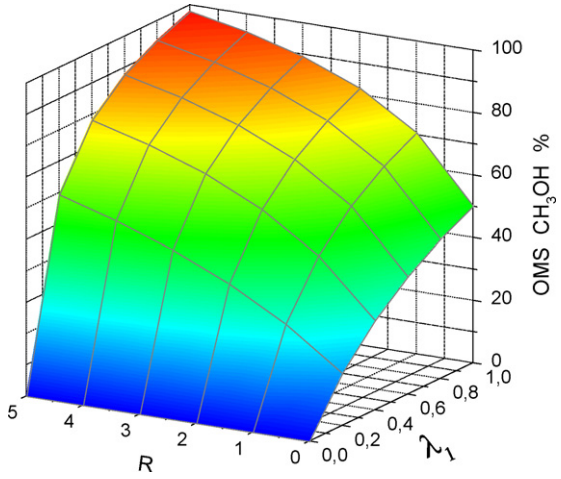

Fig. 2. Overall module selectivity to methanol (OMS_{CH_3OH}%). Thermodynamic limit; process condition E-1 (Table 1); $\lambda_2 = 1$.

process conditions, up to 89% CO_2 could be converted to CH_3OH (for $R = 5$ and $\lambda_1 = 1$), with an overall module selectivity of ≈98%. Therefore, the following analyses will be centered only on the cases for which both reactions are in equilibrium because it is intended to establish the maximum CO_2 capture that is thermodynamically feasible.

Fig. 3a and b shows the OMC_{CO_2}% and the OMS_{CH_3OH}% values for different molar H_2/CO_2 module feed ratios (conditions (E-4)–(E-6) in Table 1). The trends exposed in Fig. 3 are similar for the OMC_{H_2}%. It can be seen that both OMC_{CO_2}% and OMS_{CH_3OH}% grow steadily upon increasing the gas recycle ratio, reaching their maximum values around the stoichiometric feed ratio corresponding to the synthesis reaction (R_1), where $R = 5$.

Similar analyses varying either pressure or temperature showed that the capture of CO_2 always increases for higher values of recycle ratios upon increasing the operating pressure or decreasing the reaction temperature. Because $\Delta\upsilon_1$ is negative, the reaction can progress further at higher pressure and, likewise, because (R_1) is an exothermic reaction, the capture of CO_2 is favored at lower process temperatures (Fig. 4). In both cases, for $R = 5$ and for $P > 4$ MPa, or $T \approx 508$ K, the percentage captures of CO_2 and H_2 in the 'equilibrium reactor' could reach as high as 100%. Thus, for the quantitative comparisons that will be made with regard to OMC_{CO_2}%, using the ideal (1D) catalytic reactor in the synthesis module, only values obtained with $R = 5$ will be used so as to contrast the performance of the studied catalysts with the maximum *achievable* thermodynamic overall CO_2 capture.

3.2. The ideal 1D catalytic reactor

Table 2 details the process conditions under which the performance of the two considered catalysts was studied. Within each group of process conditions listed in this table, only one variable at a time was changed with respect to condition C-1, which will be taken as the pivot condition in the following analyses. The chosen values of pressure, temperature and module feed composition (which are typical of the methanol synthesis process) were within the range of the experimental conditions used by the abovementioned research groups for obtaining the respective kinetic models. Additionally, the range of W/F_{CO_2} values was chosen in conformity with industrial plant data [2,11].

3.2.1. Ga_2O_3–Pd/SiO_2 catalyst

In qualitative terms, the trends found with regard to CO_2 and H_2 captures upon modifying pressure, temperature or module feed

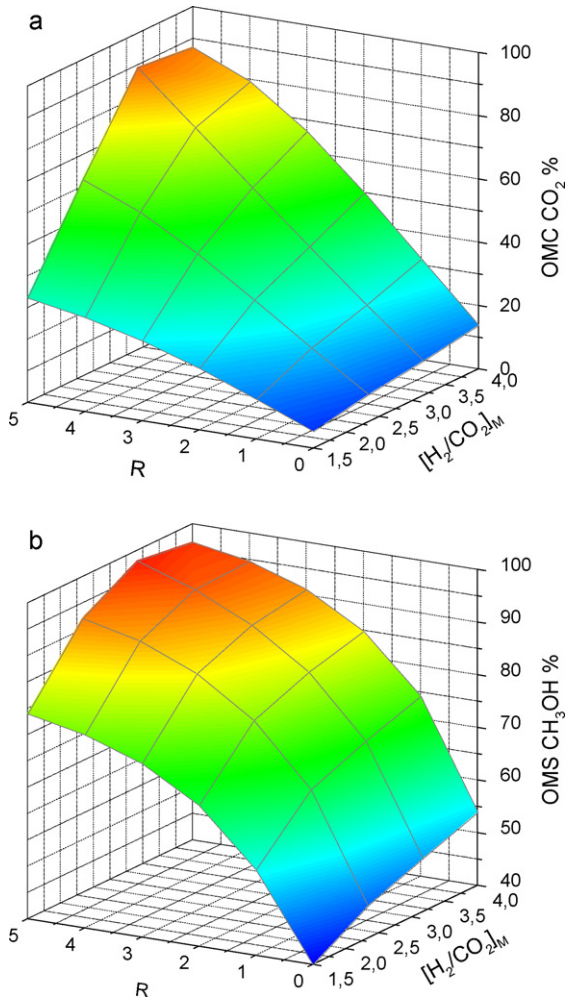

Fig. 3. (a) Overall module capture of CO_2 (OMC_{CO_2}%) and (b) overall module selectivity to methanol (OMS_{CH_3OH}%) for different module H_2/CO_2 feed ratios. Thermodynamic limit; $P = 3$ MPa; $T = 523$ K; $\lambda_1 = \lambda_2 = 1$.

composition using this catalyst when the gas recycle ratio was increased were similar to those observed by running the module with the 'equilibrium reactor' (due to space reasons, these graphs are not shown). Table 3 illustrates the extent of the changes in the overall module capture of CO_2 that would ensue from raising the

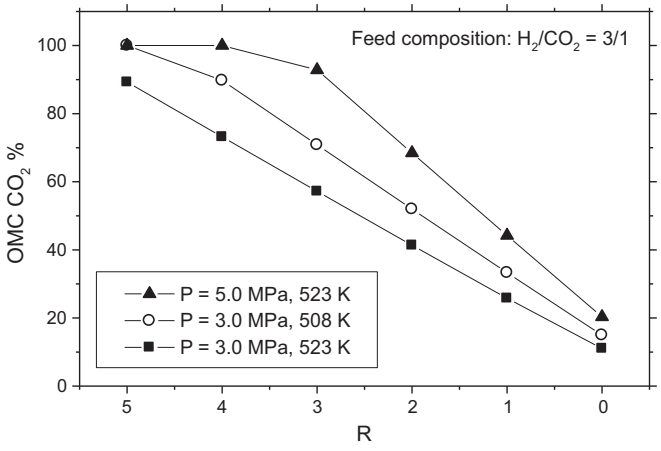

Fig. 4. OMC_{CO_2}% vs. pressure for different gas recycle ratios (R). Thermodynamic limit; $T = 523$ K; $H_2/CO_2 = 3$; $\lambda_1 = \lambda_2 = 1$.

Table 2
Process conditions studied in the 'ideal catalytic reactor' (kinetic regime).

Process condition	P (MPa)	T (K)	$[H_2/CO_2]_M$ (mol/mol)	W/F_{CO_2} (kg cat s/mol CO_2)
C-1	3	523	75/25	43.07
C-2	4	523	75/25	43.07
C-3	5	523	75/25	43.07
C-4	3	508	75/25	43.07
C-5	3	538	75/25	43.07
C-6[a]	3	523	80/20	53.83
C-7[a]	3	523	70/30	35.89
C-8[a]	3	523	60/40	26.92
C-9	3	523	75/25	107.67
C-10	3	523	75/25	21.53
C-11	3	523	75/25	14.36

[a] The same W/F_{total} that was used in C-1 (rather than the same W/F_{CO_2}) was employed.

process pressure (C-3), lowering the process temperature (C-4), augmenting the proportion of H_2 in the feed (C-6), or increasing W/F_{CO_2} (C-9) with respect to the C-1 pivot condition. Only the values corresponding to $R = 5$ are presented to show an upper limit for each one of the selected conditions. As can be recognized, the modifications of pressure and temperature did not produce significant changes in the percent OMC_{CO_2}%. The increased CO_2 capture for condition C-6 entailed, however, a lower use of H_2 by the module. The most influential variable in the OMC_{CO_2}% was the residence time of the gases inside the reactor.

Fig. 5 shows how sensitive the module was to changes in the residence time of the gases inside the reactor tubes (conditions (C-9)–(C-11)). As can be appreciated, the OMC_{CO_2}%. improved substantially the higher the R and/or W/F_{CO_2} employed. These figures were significantly lower than the ones achievable with the 'equilibrium reactor', but they nevertheless indicated that reasonable CO_2 captures could also be reached using this catalyst.

At this point, it is necessary to mention that the CO content in the reactor inlet stream (stream F) for the condition of highest W/F_{CO_2} and $R = 5$ displayed in Fig. 5 ($OMC_{CO_2}\% = 29.7$) was about 5%, whereas this content was just 1.9% for the lowest value of W/F_{CO_2} considered in the analysis ($OMC_{CO_2}\% = 14.22$). The CO mole fraction in the reacting mixture is a critical variable in the performance of Pd-containing catalysts because carbon monoxide chemisorbs strongly onto the metal, decreasing the number of active sites available for H_2 dissociation [7,9]. Therefore, although for some industrial point sources the gases used to carry out the CO_2 capture process do contain some CO ($H_2/CO_2/CO = 75/22/3$ [20]), its concentration should be kept as low as possible in the system if the Ga_2O_3–Pd/SiO_2 catalyst was used. Nevertheless, our analysis evidenced that the detrimental impact of CO on the catalytic activity of

Table 3
Overall module capture of CO_2 (OMC_{CO_2}), overall module selectivity to methanol (OMS_{CH_3OH}), and specific productivity to methanol using the Ga_2O_3–Pd/SiO_2 catalyst [9] for $R = 5$[a].

Process condition	OMC_{CO_2} (%)	OMS_{CH_3OH} (%)	P_{CH_3OH} [b] (kg CH_3OH/kg cat h)
C-1	21.7	62.5	0.11
C-3	25.8	63.1	0.13
C-4	22.7	69.1	0.11
C-5	18.5	53.7	0.09
C-6[c]	25.6	65.3	0.11
C-8[c]	13.3	55.1	0.09
C-9	29.5	64.5	0.06
C-11	14.0	64.6	0.20

[a] While keeping W/F_{CO_2} constant with respect to $R = 0$.
[b] These values are similar to the ones reported in the literature [11,20,21].
[c] The same W/F_{total} used in C-1 (rather than the same W/F_{CO_2}) was employed.

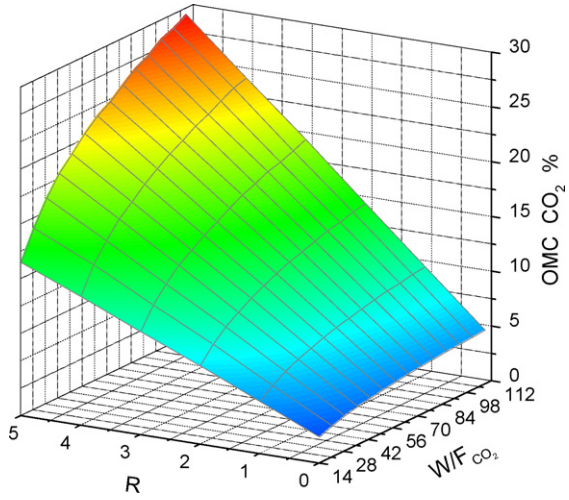

Fig. 5. OMC_{CO_2}% of the CO_2 capture module vs. W/F_{CO_2} (kg cat s/mol CO_2) using the Ga_2O_3–Pd/SiO_2 catalyst [9]. $T = 523$ K; $P = 3$ MPa; $H_2/CO_2 = 3$.

this material (appropriately incorporated in the respective kinetic expressions that were obtained by Chiavassa et al. [9]) could be conveniently counterbalanced by increasing W/F_{CO_2}.

In Table 3, the specific productivity to methanol (P_{CH_3OH}) for different operating temperatures (C-1, C-4 and C-5) is shown. For this catalyst it was apparent that any increase in the process temperature brought about a significant reduction in the productivity. Without recycling ($R = 0$), the productivity was 0.1, 0.105 and 0.085 for the conditions C-1, C-4 and C-5, respectively. This modest variation of P_{CH_3OH} upon increasing R was because, 'by design', the reactor W/F_{CO_2} in the tubes was kept constant. Indeed, the discrete change in P_{CH_3OH} achieved upon increasing R was only due to changes in the composition of the gas stream feeding the reactor tubes.

In Table 3, the variation in specific productivity for different process conditions (for $R = 5$) upon increasing the pressure (C-3), or diminishing W/F_{CO_2} (C-11), with respect to the pivot condition C-1 is shown. Although these changes in P_{CH_3OH} with pressure were moderate, it must be remembered that small improvements in the efficiency of this process can be economically significant because methanol is a valued commodity [22]. Furthermore, the election of any given process pressure aimed at obtaining high catalyst productivity has to be combined with the incremental pumping-related costs incurred by raising this operating variable. In addition, as can be judged by comparing the C-9 and C-11 entries in Table 3, the higher productivity value was achieved at the expense of the lowest CO_2 module capture of the set. There is, then, a trade-off in the selection of the residence time in the reactor.

Fig. 6 shows the overall module selectivity to CH_3OH for different recycle ratios and process temperatures. A substantial increase in OMS_{CH_3OH}% could be achieved upon increasing the gas recycle ratio, which might be attributed in part to the fact that the CO percentage in the reactor feed stream becomes higher with increasing R. This progressively prevents the RWGS from proceeding further, improving the overall module selectivity. Fig. 6 also highlights that, in order to obtain a better CO_2 capture, it was beneficial to decrease the process temperature because, whenever the selectivity to methanol was higher, the percentage of CO_2 converted into CO decreased (e.g., from 13.59% @ 523 K to 10.98% @ 508 K for $R = 5$). This phenomenon results from the difference in the activation energies between the two reactions considered because on this catalyst $\Delta E_{R2} > \Delta E_{R1}$ [9]. Incidentally, the use of a lower reaction temperature did not significantly decrease either the overall CO_2 recovery or the catalyst productivity (Table 3).

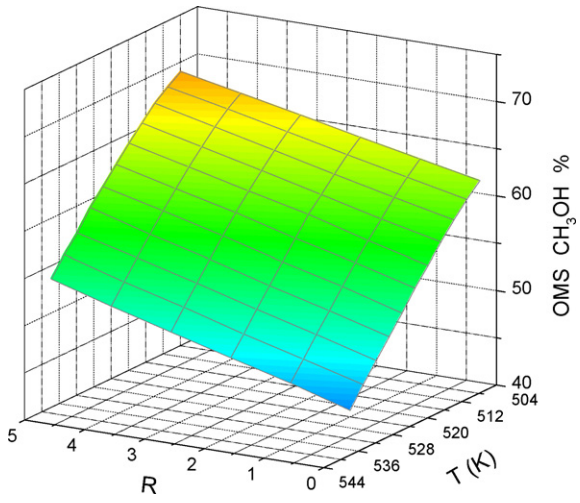

Fig. 6. OMS_{CH_3OH}% of the CO_2 capture module vs. temperature using the Ga_2O_3–Pd/SiO_2 catalyst. P = 3 MPa, H_2/CO_2 = 3, W/F_{CO_2} = 43.07 kg cat s/mol CO_2.

In Fig. 7, the OMS_{CH_3OH}% for different R and W/F_{CO_2} is presented. As can be observed, the lower selectivities corresponded to higher W/F_{CO_2} (except for R = 5). This was caused by the larger production of CO for higher residence time of the reactant gases inside the reactor.

From the former analyses it is evident that, with this catalyst and for the range of W/F_{CO_2} considered, the values of OMS_{CO_2}% and OMS_{CH_3OH}% that could be reached were well below those of the 'equilibrium reactor' for each of the process conditions that were examined, even for R = 5.

3.2.2. Commercial $CuO/ZnO/Al_2O_3$ catalyst

To make qualitative *and* quantitative comparisons regarding catalytic performance, the commercial $CuO/ZnO/Al_2O_3$ catalyst employed by Graaf et al. [13,14] was scrutinized in detail. In general, the qualitative trends with respect to CO_2 capture and specific productivity vs. process pressure, H_2/CO_2 molar feed and/or gas recycle ratios, were similar to those found with the novel material: these performance qualifiers improved by augmenting any of the abovementioned parameters. The values of OMC_{CO_2}%, OMS_{CH_3OH}% and P_{CH_3OH} for R = 5 and different process conditions are detailed in Table 4. In particular, if the pivot condition (C-1) was compared with the runs at the highest pressure (C-3) or the highest

Table 4
Overall module capture of CO_2 (OMC_{CO_2}), selectivity (OMS_{CH_3OH}), and specific productivity to methanol using the MK 101 $CuO/ZnO/Al_2O_3$ catalyst [13,14] for R = 5[a].

Process condition	OMC_{CO_2} (%)	OMS_{CH_3OH} (%)	P_{CH_3OH} (kg CH_3OH/kg cat h)
C-1	56.1	87.0	0.29
C-3	90.7	98.3	0.45
C-4	41.4	85.5	0.20
C-5	54.4	82.3	0.29
C-6[b]	59.5	87.4	0.31
C-8[b]	31.1	76.8	0.19
C-9	70.3	92.4	0.14
C-11	27.6	75.7	0.40

[a] While keeping W/F_{CO_2} constant with respect to R = 0.
[b] The same W/F_{total} used in C-1 (rather than the same W/F_{CO_2}) was employed.

H_2/CO_2 molar feed ratio (C-6) of the set, it was apparent that these last values were much higher than the ones reached using the Ga_2O_3–Pd/SiO_2 catalyst (Table 3). In contrast to the former catalyst, the process pressure now had a large influence on OMS_{CO_2}% due to the higher functional dependence of p_{CO} in the kinetics of this commercial $CuO/ZnO/Al_2O_3$ catalyst.

3.2.2.1. Impact of process temperature. The overall module capture of CO_2 showed a maximum inside the temperature interval explored (Fig. 8). This behavior was quite different from that of the novel material and of the 'equilibrium catalytic reactor', in which OMC_{CO_2}% became larger with decreasing temperature along the entire interval. As for OMS_{CH_3OH}% (Fig. 9), for low gas recycle ratios the pattern was similar to the Ga_2O_3–Pd catalyst (Fig. 6) because for this Cu/ZnO catalyst, the activation energy of the RWGS was also high (in fact, it was the highest of the three reactions considered). However, for high R, the selectivity to methanol only changed moderately, which was a result of the significant variation in the reactor feed composition when passing from low to high gas recycle ratios. This effect was also modest in the novel material given its lower catalytic activity.

It has to be noticed that, although the selectivity to methanol was much higher when T = 508 K (Fig. 9), the capture of CO_2 became the lowest, despite the gas recycle ratio (Fig. 8). This implies that (at least within the range of process conditions selected in this work,) in order to get the highest values of CO_2 capture, and also P_{CH_3OH}, it is preferable to develop highly active catalytic materials, putting less emphasis on their selectivity.

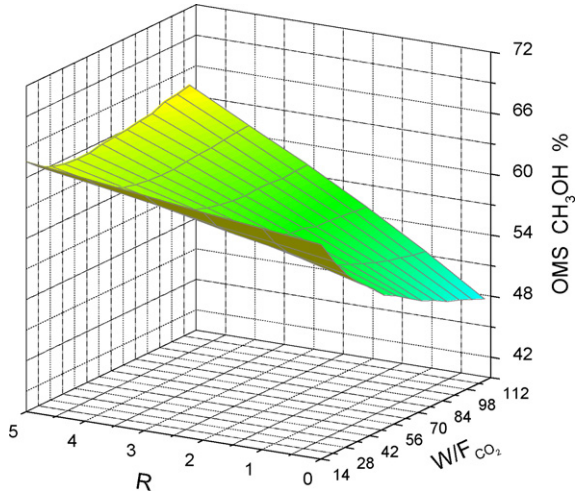

Fig. 7. OMS_{CH_3OH}% of the CO_2 capture module vs. W/F_{CO_2} (kg cat s/mol CO_2) using the Ga_2O_3–Pd/SiO_2 catalyst. P = 3 MPa; T = 523 K; H_2/CO_2 = 3.

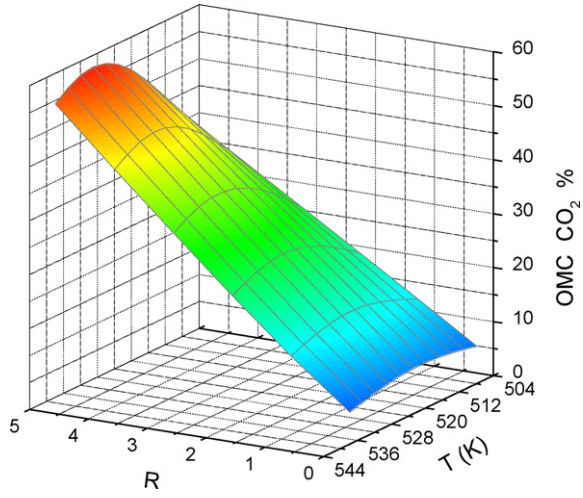

Fig. 8. OMC_{CO_2}% of the CO_2 capture module vs. temperature using the commercial $CuO/ZnO/Al_2O_3$ catalyst [13,14]. P = 3 MPa; H_2/CO_2 = 3; W/F_{CO_2} = 43.07 kg cat s/mol CO_2.

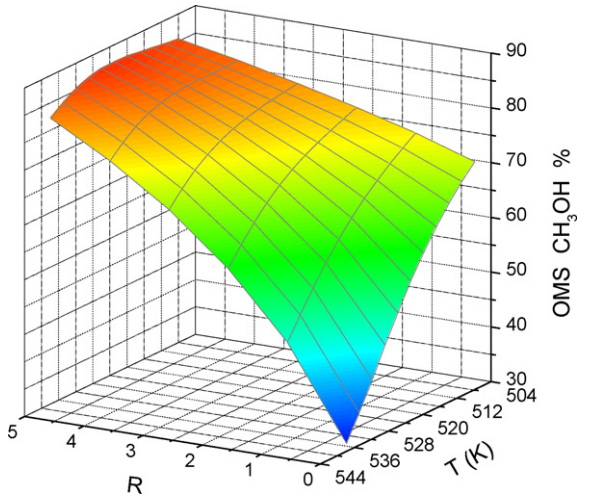

Fig. 9. OMS_{CH_3OH}% of the CO_2 capture module vs. temperature using the commercial $CuO/ZnO/Al_2O_3$ catalyst. P = 3 MPa, H_2/CO_2 = 3; W/F_{CO_2} = 43.07 kg cat s/mol CO_2.

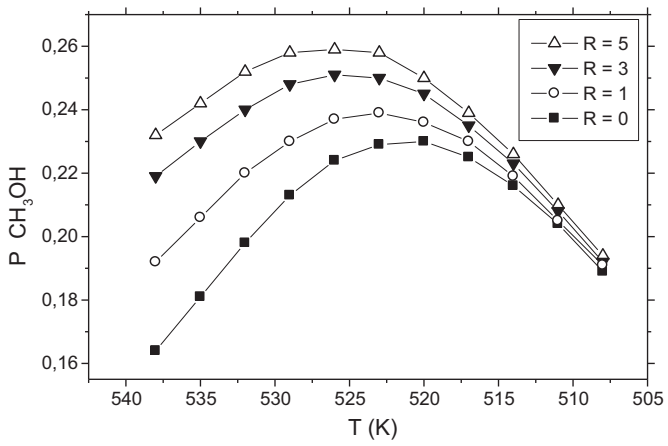

Fig. 11. Specific productivity to methanol (P_{CH_3OH}) vs. temperature using the commercial $CuO/ZnO/Al_2O_3$ catalyst in the CO_2 capture module for various gas recycle ratios and a constant W/F_{carbon} = 43.07 kg cat s/mol carbon source. P = 3 MPa; H_2/CO_2 = 3.

In Fig. 10, the specific catalyst productivity to methanol for different recycle ratios and temperatures is presented for W/F_{CO_2} = 43.07 kg cat s/mol CO_2. Unlike the novel material, the productivity rose for higher gas recycle ratios, despite the fact that W/F_{CO_2} was not changed. This was because commercial catalysts are adequate to operate with syn-gas (composition is typically $H_2/CO/CO_2$ = 69/25/6 [23]). For lower R, the catalyst, mostly fed with H_2/CO_2, produced preferably carbon monoxide, whereas for high recycle ratios (3–5) the produced CO was reincorporated into the reactor and converted to methanol, thus raising both CO_2 capture yield and selectivity of the desired product.

In regards to the maximum P_{CH_3OH} value that could be reached within the temperature interval, there were differences according to whether W/F_{CO_2} (Fig. 10) or W/F_{carbon} (Fig. 11) was chosen as the key parameter for the analysis. In every case, there was a shift in the maximum P_{CH_3OH} toward higher temperatures with increasing gas recycle ratio. This shift was larger when W/F_{CO_2} was kept constant, with a productivity maximum located at about 534 K (for R = 5). However, when W/F_{carbon} was kept constant instead, the maximum was located at 526 K. In either case, the maximum P_{CH_3OH} for R = 0 was found at 520 K. The significant difference existing between the productivity values corresponding to R = 0 and R = 5 in the high temperature region of Figs. 10 and 11 merited special attention. This observation implies that any increase of the reactor temperature set to counteract an eventual catalyst deactivation must always be accompanied by a larger gas recycle ratio if the same productivity value is to be kept.

3.2.2.2. Impact of space velocity. The residence time inside the reactor has a profound impact on OMC_{CO_2}%, as clearly shown in Fig. 12. The trends on the overall CO_2 capture upon modifying W/F_{CO_2} and/or the gas recycle ratio were quite similar using this material to the ones found with the Ga_2O_3–Pd/SiO_2 catalyst (Fig. 5). However, with the $CuO/ZnO/Al_2O_3$ catalyst the CO_2 capture was considerably higher (compare conditions C-1, C-9 and C-11 in Tables 3 and 4).

The OMS_{CH_3OH}% was always higher on this catalyst when the gas recycle ratio was increased (Fig. 13). Furthermore, for R > 1 the selectivity to methanol became higher with increasing W/F_{CO_2}. It is well known that water, together with CO_2, maintains copper in a desirable oxidation state (on Cu^{2+} oxidized sites reaction (R_1) occurs, while CO hydrogenation proceeds on Cu^+ sites [24]). However, the excess of water suppresses the hydrogenation of CO_2 because it competes with this reactant for adsorption sites [2] and also accelerates the crystallization/coalescence of Cu and ZnO [21]. At higher gas recycle ratios, though, the higher molar fraction of CO in the reactor feed stream offsets the deleterious impact of water

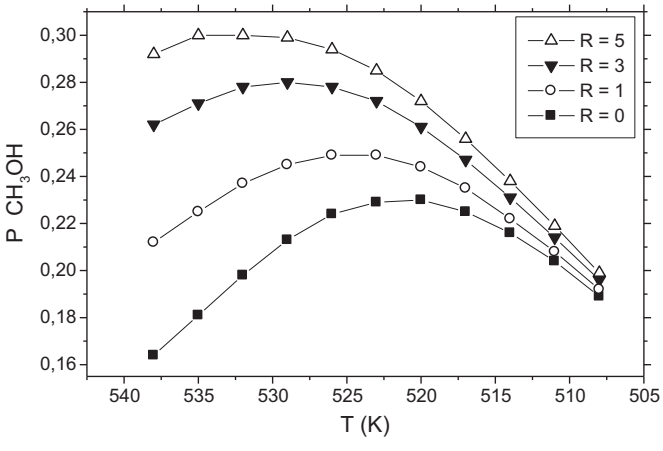

Fig. 10. Specific productivity to methanol (P_{CH_3OH}) vs. temperature using the commercial $CuO/ZnO/Al_2O_3$ catalyst in the CO_2 capture module for various gas recycle ratios and W/F_{CO_2} = 43.07 kg cat s/mol CO_2. P = 3 MPa; H_2/CO_2 = 3.

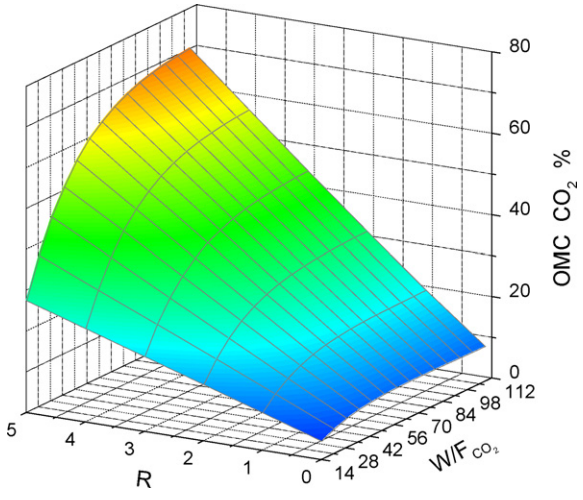

Fig. 12. OMC_{CO_2}% of the CO_2 capture module vs. W/F_{CO_2} (kg cat s/mol CO_2) using the commercial $CuO/ZnO/Al_2O_3$ catalyst. T = 523 K; P = 3 MPa; H_2/CO_2 = 3.

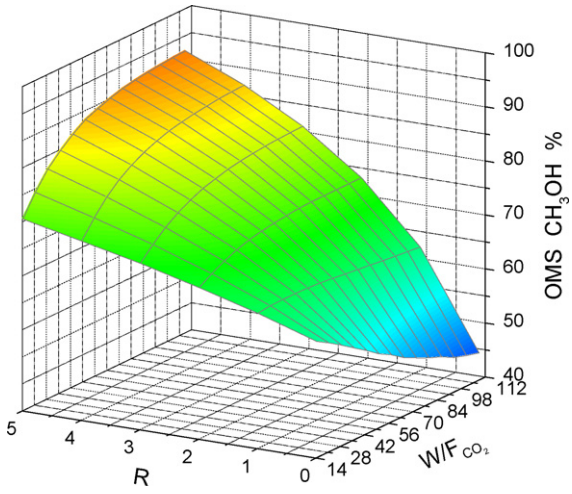

Fig. 13. OMS_{CH_3OH}% of the CO_2 capture module vs. W/F_{CO_2} (kg cat s/mol CO_2) using the commercial $CuO/ZnO/Al_2O_3$ catalyst. $T = 523$ K; $P = 3$ MPa; $H_2/CO_2 = 3$.

because CO is a key participant in methanol synthesis. This is the reason there was no selectivity improvement on the novel catalyst at higher R upon increasing W/F_{CO_2} (Fig. 7) because this catalyst is unable to convert CO into the desired products.

4. Conclusions

The capture of CO_2 from point-source emissions *via* its transformation in liquid derivatives (particularly methanol) by catalytic hydrogenation is both conceptually attractive and attainable in practical terms. If it were feasible to have catalysts for which the relevant process reactions (i.e., the hydrogenation of carbon dioxide and the reverse water gas shift reaction (RWGS)) could perform under 'near thermodynamic equilibrium conditions', overall CO_2 captures higher than 50% could be achieved, still operating within the range of pressure and temperature industrially used nowadays. Indeed, methanol synthesis modules operating with recycle ratios (R) of non-condensable gases (CO_2, CO, and H_2) equal to or larger than 3 are customarily employed in syn-gas plants. Up to 100% overall CO_2 capture could be reached using $R \approx 5$ and $P \geq 4$ MPa ($T = 523$ K) or $T = 508$ K ($P \geq 3$ MPa).

Using an ideal (isothermal, isobaric, pseudohomogeneous) 1D plug flow reactor, the performance of two catalysts, with intrinsically different characteristics but with well-described kinetics for this process, was analyzed. One of these materials was developed by our research team (Ga_2O_3–Pd/SiO_2), while the other was a commercial $CuO/ZnO/Al_2O_3$ catalyst. It was shown that attractive CO_2 captures could be achieved with some of these materials (higher than 40% for $CuO/ZnO/Al_2O_3$), but only whenever the most exacting process conditions (i.e., high pressure and gas recycle ratios) were used, particularly if the novel Pd-based material (whose specific activity was much lower than those of the commercial catalyst) was put to work. In every case, the highest CO_2 capture levels were reached for high W/F_{CO_2} values and with the highest recycle ratios of non-condensable gases.

As the conceptual logic, the economic constraints and the underlying thermodynamics of this process necessarily call for the separation of condensable vapors (CH_3OH and H_2O) and the recycle of non-condensable gases, this systematic evaluation of the impact of the relevant operating variables on the capture of carbon dioxide *via* CH_3OH synthesis indicated that, in terms of specific productivity, the efforts to improve the overall CO_2 capture of these modules should be focused on the development of highly active catalytic materials rather than achieving the highest selectivity to methanol.

Acknowledgments

The financial support of CONICET, UNL and ANPCyT (PICT 14-25282) is gratefully acknowledged by the authors.

References

[1] K. Ushikoshi, K. Mori, T. Kubota, T. Watanabe, M. Saito, Appl. Organomet. Chem. 14 (2000) 819–825.
[2] O.S. Joo, K.D. Jung, I. Moon, A.Y. Rozovskii, G.I. Lin, S.H. Han, S.J. Uhm, Ind. Eng. Chem. Res. 38 (1999) 1808–1812.
[3] O.-S. Joo, K.-D. Jung, Y. Jung, Stud. Surf. Sci. Catal. 153 (2004) 67–72.
[4] J.-P. Lange, Catal. Today 64 (2001) 3–8.
[5] G.C. Chinchen, P.J. Denny, J.R. Jennings, M.S. Spencer, K.C. Waugh, Appl. Catal. 36 (1988) 1–65.
[6] A.L. Bonivardi, D.L. Chiavassa, C.A. Querini, M.A. Baltanás, Stud. Surf. Sci. Catal. 130 (2000) 3747–3752.
[7] D.L. Chiavassa, J. Barrandeguy, A.L. Bonivardi, M.A. Baltanás, Catal. Today 133–135 (2008) 780–786.
[8] J. Barrandeguy, Master's Thesis, Universidad Nacional del Litoral, Argentina, 2002.
[9] D.L. Chiavassa, S.E. Collins, A.L. Bonivardi, M.A. Baltanás, Chem. Eng. J. 150 (2009) 204–212.
[10] K.A. Islam, W.B. Eearl, Can. J. Chem. Eng. 68 (1990) 702–704.
[11] N. Rezaie, A. Jahanmiri, B. Moghtaderi, M.R. Rahimpour, Chem. Eng. Proc. 44 (2005) 911–921.
[12] M.R. Rahimpour, S. Ghader, M. Baniadam, J. Fathikalajahi, Chem. Eng. Technol. 26 (6) (2003) 672–678.
[13] G.H. Graaf, E.J. Stamhuis, A.A.C.M. Beenackers, Chem. Eng. Sci. 43 (1988) 3185–3195.
[14] G.H. Graaf, H. Scholtens, E.J. Stamhuis, A.A.C.M. Beenackers, Chem. Eng. Sci. 45 (1990) 773–783.
[15] G.H. Graaf, P.J.J.M. Sijtema, E.J. Stamhuis, G.E.H. Joosten, Chem. Eng. Sci. 41 (1986) 2883–2890.
[16] J. Skrzypek, M. Lachowska, D. Serafin, Chem. Eng. Sci. 45 (1990) 89–96.
[17] J. Skrzypek, M. Lachowska, M. Grzesik, J. Sloczynski, P. Nowak, Chem. Eng. J. 58 (1995) 101–108.
[18] R.C. Reid, J.M. Prausnitz, T.K. Sherwood, B.E. Poling, The Properties of Gases and Liquids, 4th ed., McGraw-Hill, New York, 1987.
[19] T. Chang, R.W. Rousseau, P.K. Kilpatrick, Ind. Eng. Chem. Proc. Des. Dev. 25 (1986) 477–481.
[20] J.S. Lee, K.H. Lee, S.Y. Lee, Y.G. Kim, J. Catal. 144 (1993) 414–424.
[21] F. Gallucci, A. Basile, Int. J. Hydrogen Energy 32 (2007) 5050–5058.
[22] C.J. Schack, M.A. McNeil, R.G. Rinker, Appl. Catal. 50 (1989) 247–263.
[23] J. Wu, M. Saito, M. Takeuchi, T. Watanabe, Appl. Catal. A: Gen. 218 (2001) 235–240.
[24] G.A. Vedage, R. Pitchat, R.G. Herman, K. Klier, Proc. 8th. Int. Congr. Catalysis, vol. II, Verlag-Chemie, Berlin, Weinheim, 1984, pp. 47–58.